J. Fluid Mech. (1975), *vol.* 71 *part* 2, *pp.* 407–415
Printed in Great Britain

The development of a partially mixed region in a stratified shear flow

By R. J. HARTMAN
Department of Physics, University of California, Santa Barbara

(Received 16 October 1974)

The influence of a mean uniform shear on the development of a partially mixed region in an unbounded stratified fluid is considered. Results are given for the very near field and the far field in the large-J (Richardson number) limit. A qualitative discussion for $J \gtrsim 1$ is also included. The near-field motion is modified on a time scale given by $R\tau \sim J^{-\frac{1}{4}}$, where $R = dU/dz$ is the mean shear strength. This modification is shown to be a consequence of the kinematic distortion of the wake profile by the mean shear. The radiation field is largely anticipated by the wave-packet discussion of an earlier paper.

1. Introduction

The problem of the dynamical development of an initially mixed region (wake) in a density-stratified fluid has already received experimental (Schooley & Stewart 1963; Wu 1969) and theoretical (Mei 1969; Miles 1971; Hartman & Lewis 1972) attention. In flows of geophysical and astrophysical interest, stratification is invariably accompanied by an imposed shear, which, presumably, alters the basic features of the development considerably. We have therefore chosen a particularly simple model which permits extensive analytical analysis in an effort to isolate the principal effects of such an imposed shear.

The initial-value approach of an earlier paper (Hartman 1975, designated hereafter as I) is the basis for our treatment. The notation and basic flow of that paper are adopted without comment. We give the near-field and radiation-field development of the initial perturbation considered by Hartman & Lewis (1972). The radiation field is anticipated by the wave-packet discussion of I and the zero-shear results of Hartman & Lewis. The near field exhibits several unusual features, which are discussed in the body of the paper. We limit our discussion primarily to the weak-shear (large-J) regime, although some conclusions for $J \gtrsim 1$ can be drawn.

2. The initial-value problem

We adopt the basic flow, notation and several of the results of I without comment. We choose the initial wake geometry and initial conditions of Hartman & Lewis (1972):

$$\mathbf{v}(\mathbf{x}, t = 0) = 0, \quad \rho(\mathbf{x}, t = 0) = \begin{cases} \epsilon z & (r \leqslant a), \\ 0 & (r > a). \end{cases} \tag{2.1}$$

Here r is the radius from the origin and we tacitly assume $\epsilon \ll |d\rho_0/dz|$ to permit a linear analysis. The initial conditions on the vorticity ζ follow from (2.1) and the linearized vorticity equation (in convected co-ordinates)

$$\frac{\partial \zeta}{\partial \tau} = \frac{-g}{\rho_{00}} \frac{\partial \rho}{\partial \xi}. \tag{2.2}$$

The Fourier-transformed initial conditions on ζ follow from (2.2) and the Fourier transform of (2.1),

$$\tilde{\rho}(\mathbf{k}, t=0) = -2\pi i \epsilon (a^2/k) J_2(ka) \sin\theta. \tag{2.3}$$

Here J_n is a Bessel function of order n, (k, θ) represents the polar co-ordinate decomposition of the Fourier component $\mathbf{k}$ and we measure all angles counter-clockwise from $\hat{\mathbf{x}}$. The solution to the initial-value problem for ζ now follows from the Fourier inversion integral (I, 2.13), while the solution for the stream function ψ follows from (I, 2.10). We have

$$\psi(\boldsymbol{\xi}, \tau) = \frac{1}{2\pi} \frac{\epsilon a^2 g}{N\rho_{00}} \int_0^\infty dk \int_0^{2\pi} d\theta \frac{J_2(ka)}{k} \frac{\sin\theta}{\cos\theta} \exp\left[ikr\cos(\theta-\alpha)\right] \frac{f_m(\tau,\theta)}{1+T^2} \sin\left[\gamma(\tau,\theta)\right], \tag{2.4}$$

where

$$f_m(\tau,\theta) = [1+T^2]^{\frac{1}{4}}\,[1+T^2(0)]^{\frac{1}{4}}, \tag{2.5a}$$

$$\gamma(\tau,\theta) = J^{\frac{1}{2}} \ln\left[\frac{T+(1+T^2)^{\frac{1}{2}}}{T(0)+(1+T^2(0))^{\frac{1}{2}}}\right], \tag{2.5b}$$

$$T = R\tau - \tan\theta, \quad T(0) = -\tan\theta. \tag{2.5c, d}$$

We use the polar representation (r, α) for field points in convected co-ordinates and we shall not, for the most part, transform our analytic results back into unconvected (laboratory) co-ordinates, although the inverse transform to (I, 2.7) may be performed without difficulty. Our problem is now reduced to the evaluation of (2.4).

3. The near field

In 'laboratory', or unconvected, co-ordinates the basic wake profile is kinematically deformed in time into an ellipse whose semimajor axis makes an angle

$$\tan^{-1}\left[-\tfrac{1}{2}Rt + (1+\tfrac{1}{4}R^2t^2)^{\frac{1}{2}}\right] \tag{3.1a}$$

with the horizontal. The length of the semimajor axis is

$$A = a\left[1 + R^2t^2 + Rt(1+\tfrac{1}{4}R^2t^2)^{\frac{1}{2}}\right]^{\frac{1}{2}} \tag{3.1b}$$

and that of the semiminor axis is $B = a^2/A$. As $t \to 0$ the profile becomes nearly circular with its semimajor axis at 45° to the horizontal. As time proceeds the ellipse elongates and rotates, becoming for $Rt \gg 1$ a thin, nearly horizontal sheet. (See also figure 1.) In the convected co-ordinate system, the basic circular outline of the initial perturbation does not change and we may consider $r > a$ and $r < a$ separately. The integral over k occurring in (2.4) is of the Weber–Shafheitlin form and may be evaluated exactly (HMF, equations 11.4.35 ff.†).

† We use the terminology and notation of Abramowitz & Stegun (1970, herein denoted by HMF).

For $r < a$ the remaining integral over θ may be evaluated, for $Nt \gg 1$, by standard stationary-phase procedures. This evaluation is complicated slightly by the occurrence of two independent parameters (J and $R\tau$) in the phase $\gamma(\tau, \theta)$. We therefore give a brief sketch of our analysis.

We have, as an exact result up to this point,

$$\psi(\xi, \tau) = -\frac{1}{2\pi}\frac{\epsilon g r^2}{N\rho_{00}}\int_{-\frac{1}{2}\pi}^{\frac{1}{2}\pi} d\theta \cos^2(\theta-\alpha)\sin\theta\left[\frac{1+T^2(0)}{1+T^2}\right]^{\frac{3}{4}}\sin[\gamma(\tau,\theta)], \quad (3.2)$$

where a spatially constant term, irrelevant to the velocity fields, has been dropped. For J large we may easily obtain the first term of an asymptotic expansion of (3.2) by the usual stationary-phase procedure, provided that $R\tau$ is not small. When $R\tau \ll 1$ we have

$$\gamma(\tau, \theta) = Nt\cos\theta(1+O(R\tau)),$$

which still allows a stationary-phase asymptotic evaluation in $1/Nt$. We note here that such asymptotic series can generally be expected to give quite good qualitative results even for $J \gtrsim 1$ and $N\tau \gtrsim 1$ respectively. Also, since $N\tau = J^{\frac{1}{2}}R\tau$, it is not inconsistent to consider $N\tau$ large while $R\tau \ll 1$. For $N\tau$ not necessarily large, the integrand in (3.2) may be expanded in a power series in $R\tau$ and the coefficients computed exactly. The results of these evaluations may be conveniently summarized as follows:

$$\psi(\xi, \tau) = \frac{-\epsilon g}{2\rho_{00}N}\left\{4\xi\eta\frac{J_2(N\tau)}{N\tau} + \frac{R\tau}{2}\xi^2 J_1(N\tau)\right\}\{1+O(J^{-\frac{1}{2}})\}$$

$$\text{for} \quad 0 \leqslant R\tau \leqslant J^{-\frac{1}{4}} \quad \text{(early stage)}; \quad (3.3a)$$

$$\psi(\xi, \tau) = \frac{\epsilon g}{2\rho_{00}N}\left(1+\frac{R^2\tau^2}{4}\right)^{-\frac{7}{4}}\left[\frac{2}{\pi N\tau}\right]^{\frac{1}{2}}\left\{\frac{4\xi\eta\cos\Omega(\tau)}{N\tau(1+\frac{1}{4}R^2\tau^2)^{\frac{1}{2}}} - \frac{R\tau}{2}\left(\xi+\frac{R\tau}{2}\eta\right)^2\sin\Omega(\tau)\right\}$$

$$\times\{1+O(J^{-\frac{1}{2}})\} \quad \text{for} \quad R\tau \geqslant J^{-\frac{1}{4}} \quad \text{(late stage)}. \quad (3.3b)$$

Here $$\Omega(\tau) \equiv 2J^{\frac{1}{2}}\ln[\tfrac{1}{2}R\tau + (1+\tfrac{1}{4}R^2\tau^2)^{\frac{1}{2}}] - \tfrac{1}{4}\pi.$$

In (3.3a), all terms $O(R^2\tau^2)$ have been omitted since these are necessarily $O(J^{-\frac{1}{2}})$. We note that for $N\tau \sim 1$ the coefficient of $R\tau$ in (3.3a) is in error in the sense that the validity of this term (and this term only) is limited to $N\tau \gg 1$ as described earlier. For $N\tau \sim 1$, however, this erroneous contribution is $O(J^{-\frac{1}{2}})$ so the error does not manifest itself at our level of approximation.

The stream function (3.3) is seen to consist of two distinct parts. The first term, which dominates the $R\tau < J^{-\frac{1}{4}}$ behaviour, is just the irrotational zero-shear result of Hartman & Lewis. The second term, which dominates the $R\tau > J^{-\frac{1}{4}}$ development, is a rotational term, giving rise to a uniform vorticity throughout the wake, and has no counterpart in the zero-shear problem. In fact, either by following the procedure used to obtain (3.3) or more simply by operating on (3.2) with the Laplacian, we have for all $N\tau \gg 1$ (and qualitatively for $N\tau \gtrsim 1$)

$$\zeta(\xi, \tau) = -\frac{\epsilon g}{N\rho_{00}}\frac{R\tau}{2}\left(1+\frac{R^2\tau^2}{4}\right)^{-\frac{3}{4}}\sin\Omega(\tau)\{1+O(J^{-\frac{1}{2}})\}. \quad (3.4)$$

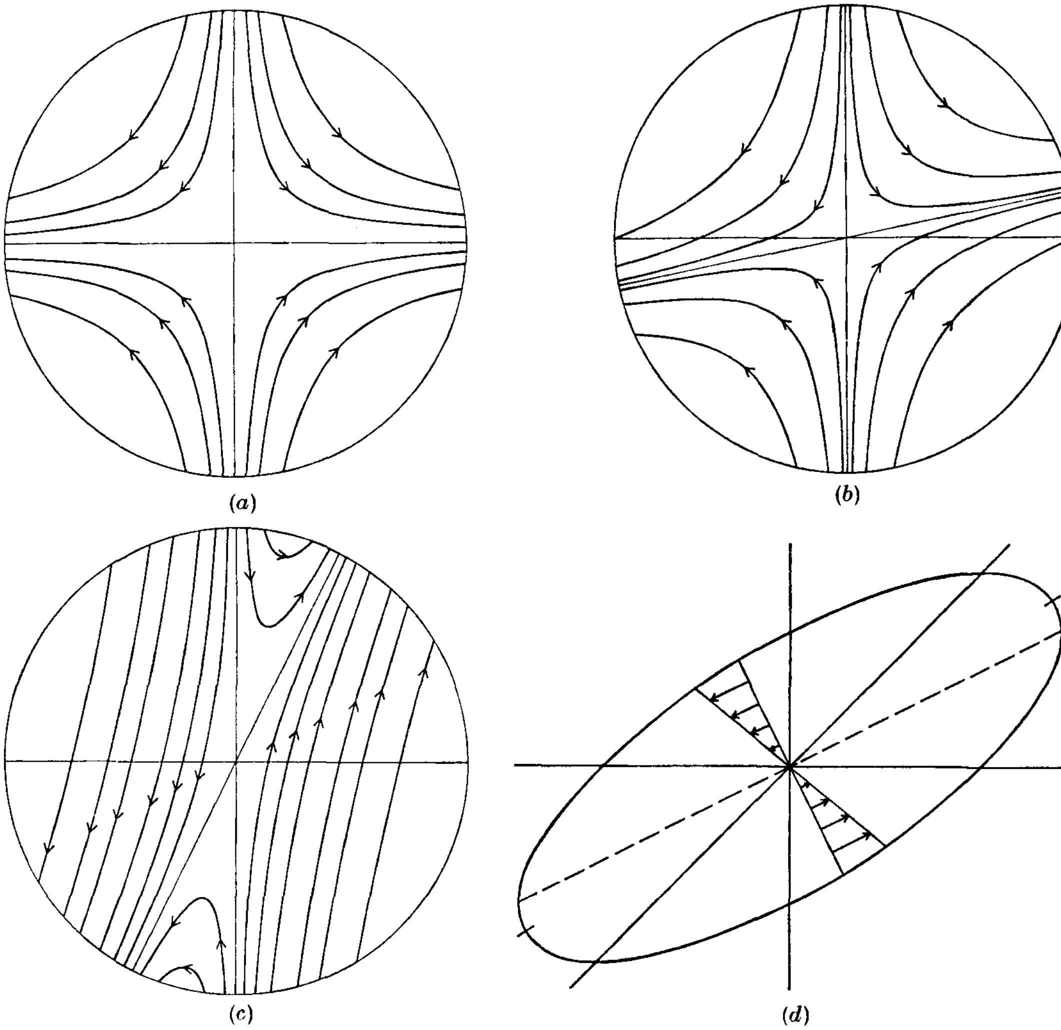

Figure 1. The perturbed streamlines, viewed in 'laboratory' co-ordinates, as given by (3.3). (a) $R\tau = 0{\cdot}3\, J^{-\frac{1}{4}}$. (b) $R\tau = 1{\cdot}3\, J^{-\frac{1}{4}}$. (c) $R\tau = 4\, J^{-\frac{1}{4}}$. (d) $R\tau = 1$. In (d) the solid line represents the position of an initially vertical fluid line element, the (unpictured) streamlines inside the wake boundary are parallel to the dashed line, and the arrows depict the direction and magnitude of the perturbed velocity. The ticks mark the semimajor axis of the ellipse [see (3.1 a, b)].

In the very early stages of collapse ($R\tau \ll J^{-\frac{1}{4}}$), the shape of the streamlines (and particle paths) is given by the irrotational right-hyperbolic form of the zero-shear problem (figure 1a). As $R\tau \to J^{-\frac{1}{4}}$ the streamlines remain hyperbolic but the initially horizontal asymptotes of the hyperbolas rotate towards the vertical (figure 1b, c). For $R\tau \sim 1$ the influence of the irrotational field is negligible and we are left with a uniform oscillating shear perturbation (figure 1d). It is emphasized that the drastic alteration of the basic flow structure illustrated in figure 1 occurs on a sufficiently short time scale ($R\tau \sim J^{-\frac{1}{4}}$) that the initially circular wake profile (viewed in laboratory co-ordinates) remains unchanged.

The behaviour of the total wake energy is also of interest. In the early stage, energy in the form of internal waves is radiated copiously and appears in the radiation field (§4). By the time $R\tau \sim J^{-\frac{1}{4}}$, the wake retains only a fraction $O(J^{-\frac{3}{4}})$ of the initial perturbation energy. However, it is easily verified from (3.3*b*) that for $R\tau > J^{-\frac{1}{4}}$ the total wake energy *increases* to a maximum when $R\tau = \sqrt{2}$. At this point, the total energy is a fraction $O(J^{-\frac{1}{2}})$ of the initial ($t = 0$) energy, an increase $O(J^{\frac{1}{4}})$ over the wake energy minimum occurring near $R\tau = J^{-\frac{1}{4}}$.

The wake energy balance in the regime $R\tau \sim 1$ consists of two sometimes conflicting contributions: internal wave radiation, evidenced by the factor $(N\tau)^{-\frac{1}{2}}$ in (3.3*b*), and the transfer of energy between the wake and the mean flow, evidenced by the amplitude factor $(\xi + \frac{1}{2}R\tau\eta)^2 R\tau/(1+\frac{1}{4}R^2\tau^2)^{\frac{7}{4}}$. For $R\tau \lesssim \sqrt{2}$, Reynolds stresses transfer energy from the mean flow to the wake faster than it can be radiated away. For $\sqrt{2} < R\tau < 2\sqrt{2}$, the internal wave radiation overcomes the flow–wake transfer, while for $R\tau > 2\sqrt{2}$ both the radiative effects and the Reynolds stresses act to reduce the wake energy. A detailed analysis of the Reynolds stresses for this problem will not be given.

It is interesting that the shearing perturbation of (3.3*b*) and figure 1(*d*) is a relatively ineffective radiator of internal waves. The flow due to the initial perturbation

$$\mathbf{v}(t=0) = 0, \quad \rho(t=0) = \begin{cases} \epsilon x & (r \leqslant a), \\ 0 & (r > a), \end{cases} \tag{3.5}$$

which generates a shearing motion similar to that in figure 1(*d*), can, in the absence of shear ($R = 0$), be obtained after the manner of Hartman & Lewis (1972). The result,

$$\rho(\mathbf{x}, t) = 2\epsilon x[J_0(Nt) - J_1(Nt)/Nt] \quad (r < a),$$

demonstrates clearly the relatively slow $(Nt)^{-\frac{1}{2}}$ decay of this perturbation compared with the $(Nt)^{-\frac{3}{2}}$ asymptotic behaviour in the Hartman–Lewis problem.

It is also worthwhile to note that perturbations of the form (2.3), which at $t = 0$ cluster Fourier wave vectors near the vertical, grow especially effectively (for $R\tau \lesssim 1$) at the expense of the mean flow. Perturbations of the form (3.5), which cluster wave vectors near the horizontal, grow much less vigorously, if at all, for $R\tau \lesssim 1$. All perturbation energy is ultimately absorbed into the mean flow regardless of the form of the initial disturbance. These observations follow directly from the comments on wave-packet energetics given in I along with a consideration of the distribution of wave vectors in the initial perturbation.

For $J \gtrsim 1$ our analysis is, strictly speaking, invalid. However, we can still expect qualitatively good results from our saddle-point evaluations, as mentioned earlier, provided that $N\tau \gtrsim 1$. For very small times we may resort to an expansion of (2.4) in powers of $R\tau$. The primary difference between $J \gtrsim 1$ and $J \gg 1$ is that the transition between the early and late stages occurs near $R\tau = 1$, when the circular wake profile is also being strongly modified by the mean shear (figure 1*d*). Also of importance is the fact that, for $J \gtrsim 1$, there is insufficient time for significant internal wave radiation to occur, so that a much larger fraction of the initial perturbation energy is ultimately absorbed *locally* by the mean flow. Qualitatively, however, the fluid motion is given adequately in this regime by the illustrations in figure 1, supplemented by an appropriately distorted wake profile in accord with the above comments.

It is perhaps of academic interest to note that the imposed shear does affect slightly the surprising discontinuous behaviour of the density and velocity fields found by Hartman & Lewis near $r = a$. It may be shown that the velocity perturbation near the original discontinuity $r = a$ *exactly* satisfies

$$v_z(r \to a_-) - v_z(r \to a_+) = -\frac{\epsilon g \eta}{N\rho_{00}} \frac{f_m(\tau, \alpha)}{1+T^2} \sin \gamma(\tau, \alpha), \tag{3.6}$$

a peculiarity of the linearized inviscid model and the discontinuous initial condition. It should be noted that, in contrast to the zero-shear behaviour, the presence of shear does cause a slow asymptotic decay of the discontinuity, again a consequence of the ultimate absorption of *all* perturbation energy by the mean flow. For comparison, the result for this discontinuity found by Hartman & Lewis in the zero-shear case is, in our notation,

$$v_z(r \to a_-) - v_z(r \to a_+) = -\frac{\epsilon g z \cos \alpha}{N\rho_{00}} \sin (Nt \cos \alpha). \tag{3.7}$$

It is important to appreciate that here, as in the wave-packet analysis of I, the principal effect of an imposed shear is kinematic. Apart from the energy transfer induced by the Reynolds stresses mentioned above, the central results of this paper can be understood qualitatively by considering at each instant an unsheared flow whose wake parameters (shape and density distribution) are determined from the kinematic distortion of the $t = 0$ wake by the mean flow. To illustrate this point we show, in appendix B, how the onset of the rotational secondary motion of (3.3*a*) may be simply understood from such a quasi-static analysis.†

4. The radiation field

The evaluation of the integrals (2.4) in the radiation zone $r/a \gg 1$ is non-standard and we outline the necessary steps in appendix A.

For $r/a \gg 1$ we find, in the convected co-ordinate system,

$$\psi(\xi, \tau) = -\frac{\epsilon a^3 g}{N\rho_{00}} \frac{\cot \alpha}{R(\tau, \alpha)} J_2\left(\frac{R(\tau, \alpha)}{r}\right) \left[\frac{f_m(\tau, \theta) \sin \gamma(\tau, \theta)}{1+T^2}\right]_{\theta=\alpha+\frac{1}{2}\pi}, \tag{4.1}$$

where
$$R(\tau, \alpha) = \frac{aJ^{\frac{1}{2}}}{\sin^2 \alpha} \left[\frac{1}{(1+T^2(0))^{\frac{1}{2}}} - \frac{1}{(1+T^2)^{\frac{1}{2}}}\right]_{\theta=\alpha+\frac{1}{2}\pi} \tag{4.2}$$

and f_m, γ and T are given in (2.5). From (I, 4.6), $R(\tau, \alpha)$ is seen to be the position of a wave group centred initially at $r = 0$ with a central wave vector of magnitude $k_0 = 1/a$ and direction $\theta_k = \alpha + \frac{1}{2}\pi$. Such a wave packet propagates in the $\hat{\theta}_k$ direction, that is, along the line joining the origin and the field point (r, α). Thus (4.1) represents an outward-travelling pulse of radiation whose maximum is near

† That the development of the asymptotic rotational wake behaviour is not in some way a consequence of the discontinuous initial condition, as is the feature (3.7), may be seen by applying our procedure to a similar, but continuous initial perturbation. The Gaussian perturbation $\rho(\mathbf{x}, t = 0) = \epsilon z \exp(-r^2/a^2)$ is especially useful in this respect.

$r = R(\tau, \alpha)$ and which, upon passing a given field point (r, α), oscillates with phase $\gamma(\tau, \alpha + \frac{1}{2}\pi)$ and grows or decays with amplitude

$$f_m(\tau, \alpha + \tfrac{1}{2}\pi)\, J_2(R(\tau, \alpha)/r)/[R(\tau, \alpha)(1+T^2)].$$

It should be pointed out that the results of this section have been largely anticipated by the zero-shear study of Hartman & Lewis, together with the wave-packet analysis of I. We also note that, as always, the amplitude factor $f_m(\tau, \alpha + \frac{1}{2}\pi)/(1+T^2)$ arises from the perturbation-flow energy transfer, while the factor $J_2(R(\tau, \alpha)/r)/R(\tau, \alpha)$ represents the naturally occurring (zero-shear) amplitude decay after the passage of the initial pulse.

5. Summary and conclusions

We have used the initial-value approach of I, along with the large-J results (I, 3.6), to consider the influence of an imposed mean shear on the wake collapse problem of Hartman & Lewis. In laboratory co-ordinates, an initially circular wake profile is distorted into an ellipse whose semimajor axis grows and rotates towards the horizontal on a time scale set by the shear strength. The near-field wake dynamics separate naturally into two intervals: $R\tau < J^{-\frac{1}{4}}$ and $R\tau > J^{-\frac{1}{4}}$. In the early stage, the motion is largely irrotational with a slowly growing rotational component. The irrotational component is essentially the zero-shear motion of Hartman & Lewis, and decays rapidly owing to internal wave radiation. The rotational component is shown in appendix B to be a consequence of the kinematic distortion of the original perturbation by the mean shear. The rotational component continues to grow, partly at the expense of the irrotational perturbation and partly at the expense of the mean flow. For $R\tau > J^{-\frac{1}{4}}$ it completely dominates the fluid motion in the wake. The wake energy during the late stage grows to a maximum at $R\tau = \surd 2$. After $R\tau = 2\surd 2$, both wave radiation and Reynolds stresses serve to reduce the amplitude of the motion. The influence of mean shear on the model-characteristic discontinuous behaviour found by Hartman & Lewis near $r = a$ was noted.

In the far (radiation) field, the motion is mostly anticipated by the wave-packet discussion in I and contains no surprises.

This work was supported in part by the Advanced Research Projects Agency of the Department of Defense under Grant DA-ARO-D-31-124-72-G181.

Appendix A

As in § 3, the integral over k occurring in (2.4) may be evaluated exactly. We find, limiting ourselves to ψ for convenience and employing several straightforward trigonometric substitutions,

$$\psi(\xi, \tau) = (\epsilon a^2 g/\pi N \rho_{00})\,[I_1 + I_2], \tag{A 1}$$

where
$$I_1 = \frac{1}{2}\int_{-\sin^{-1}\beta}^{\sin^{-1}\beta} d\zeta \left[1 - 2\frac{r^2}{a^2}\sin^2\zeta\right]\frac{f_m(\tau,\theta)}{1+T^2}\tan\theta\,\sin\gamma(\tau,\theta), \tag{A 2}$$

$$I_2 = -\frac{1}{2}\int_{-\cos^{-1}\beta}^{\cos^{-1}\beta} d\phi\,\frac{f_m(\tau,\theta)\tan\theta\,\sin\gamma(\tau,\theta)}{(1+T^2)\,[(ra^{-1}\cos\phi + (r^2a^{-2}\cos^2\phi - 1)^{\frac{1}{2}}]^2}, \tag{A 3}$$

$\beta = a/r \ll 1$, $\zeta = \theta - \alpha - \frac{1}{2}\pi$ and $\phi = \theta - \alpha$. Using the smallness of β to write $\sin\beta \sim \beta$ and expanding the integrand of (A 2) about $\zeta = 0$, we find

$$I_1 = \left[\frac{f_m(\tau,\theta)}{1+T^2}\sin\gamma(\tau,\theta)\tan\theta\right]_{\theta=\alpha+\frac{1}{2}\pi} I_3\left\{1+O\left(\frac{a}{r}\right)\right\}, \qquad \text{(A 4a)}$$

where
$$I_3 = \frac{2a}{r}\left\{\frac{4a}{R(\tau,\alpha)}j_1\left[\frac{R(\tau,\alpha)}{r}\right] - j_0\left[\frac{R(\tau,\alpha)}{r}\right]\right\} \qquad \text{(A 4b)}$$

and j_n is an nth-order spherical Bessel function.

In evaluating I_2 it is important to use the fact that the integrand is appreciable only near the end points $\phi = \pm\cos^{-1}\beta$. Using some trigonometrical rearrangement, expanding the integrand about the end points and employing the substitution $(r/a)\cos\phi = \cosh s$, we have

$$I_2 = -\left[\frac{f_m(\tau,\theta)}{1+T^2}\sin\gamma(\tau,\theta)\tan\theta\right]_{\theta=\alpha+\frac{1}{2}\pi} I_4\left\{1+O\left(\frac{a}{r}\right)\right\}, \qquad \text{(A 5a)}$$

where
$$I_4 = \int_0^\infty ds(e^{-s}-e^{-3s})\cos\left[\frac{R(\tau,\alpha)}{r}\cosh s\right]. \qquad \text{(A 5b)}$$

Now I_4 may be evaluated exactly using Cauchy's theorem on the rectangular strip $0 \to \infty \to \infty + i\pi \to i\pi \to 0$ in the complex s plane. We find

$$I_4 = \frac{2a}{r}\left\{\frac{4a}{R(\tau,\alpha)}j_1\left[\frac{R(\tau,\alpha)}{r}\right] - j_0\left[\frac{R(\tau,\alpha)}{r}\right] - \frac{\pi a}{R(\tau,\alpha)}J_2\left[\frac{R(\tau,\alpha)}{r}\right]\right\}. \qquad \text{(A 6)}$$

The remarkable cancellation of terms leading to (4.1) probably indicates that we have not, in fact, discovered the most expeditious procedure for the far-field evaluation of (2.4).

Appendix B

Consider the initial perturbation

$$\rho(\mathbf{x}, t=0) = \epsilon z[H(a-r) + \sigma\cos^2(\alpha - \tfrac{1}{4}\pi)\,\delta(a-r)], \qquad \text{(B 1)}$$

which represents a slightly distorted wake profile, essentially like (2.1). Here H is the Heaviside unit step function and δ the Dirac delta function. The perturbation (B 1) is an accurate representation of the profile (2.1) after a *kinematic* (mean-shear induced) distortion occurring over a period $R\tau = \sigma \ll 1$ [see (3.1)]. The development of this perturbation, in the absence of shear, can easily (and exactly) be calculated by the method given in § 3. We find, for $r < a$,

$$\rho(\mathbf{x},t) = 2\epsilon\left\{z\frac{J_1(Nt)}{Nt} + \sigma x\left[J_0(Nt) - 5\frac{J_1(Nt)}{Nt} + 12\frac{J_2(Nt)}{(Nt)^2}\right]\right\}. \qquad \text{(B 2)}$$

The first term in (B 2) is simply the undistorted (irrotational) wake result of Hartman & Lewis. The second term represents, in view of (2.2), a vorticity-creating or rotational contribution which vanishes at $t = 0$ and which is proportional to σ. The growth of the rotational component of (3.3a) (evidenced by the amplitude factor $R\tau$) is thus seen to be a kinematic effect of the distortion of the initially circular wake profile.

REFERENCES

ABRAMOWITZ, M. & STEGUN, I. A. 1970 *Handbook of Mathematical Functions*. Washington: Nat. Bur. Stand.

HARTMAN, R. J. 1975 *J. Fluid Mech.* **71**, 89.

HARTMAN, R. J. & LEWIS, H. W. 1972 *J. Fluid Mech.* **51**, 613.

MEI, C. C. 1969 *12th Int. Congr. Appl. Mech.*, pp. 321–330. Springer.

MILES, J. W. 1971 *Geophys. Fluid Dyn.* **2**, 63.

SCHOOLEY, A. H. & STEWART, R. W. 1963 *J. Fluid Mech.* **9**, 83.

WU, J. 1969 *J. Fluid Mech.* **35**, 531.